

Chapter 4

Influence of Sodium Carboxymethylcellulose on the Aggregation Behaviour of Aqueous 1-Hexadecyl-3-methylimidazolium Chloride (C₁₆MeImCl) Solutions

4.1 Introduction

Solutions comprising of polyelectrolytes and oppositely charged surfactants exhibit a rich and intricate self-aggregation behaviour.¹⁻⁸ Such a behaviour owes its origin to the strong interactions between the oppositely charged polyelectrolytes and surfactants when simultaneously present in a solution. These interactions have been attributed to the subtle interplay of electrostatic forces between the surfactant ions and the polyion, and hydrophobic forces between the hydrocarbon tails of amphiphile ions. Because of the widespread domestic, industrial, and technological applications of polyelectrolyte-surfactant mixtures during the past decades,²⁻⁶ *e.g.*, in detergency, cosmetics, and drug delivery, enhanced oil recovery, paints, pharmaceuticals, biomedical application, food and mineral processing, considerable attention has been paid to these systems.

Recent years have witnessed⁹⁻¹⁷ an upsurge of interest in the self-aggregation aptitude of a new class of ionic liquids, known as the surface active ionic liquids. This is because of the possibility of fine-tuning of the hydrophobicity of surface active ionic liquid molecules by varying the length of the alkyl chains, the type of the head-group or the nature and size of the counterions which might permit the modulation of the structure and the delicate dynamics of their micellar aggregates for specific purposes. It is, however, worth noting that although the systems consisting of polyelectrolytes and the so-called conventional surfactants have been extensively investigated,¹⁻⁸ those comprising polyelectrolytes and surface active ionic liquids, to the best of our knowledge, remained almost overlooked. The addition of oppositely charged polyelectrolytes to surface active ionic liquid solutions is expected to open up fascinating possibilities in the manipulation of material properties of polyelectrolyte-surface active ionic liquid systems on a molecular scale. This might be particularly useful in assessing the possible role of polyelectrolytes in modulating the known antimicrobial activity of surface active ionic liquids.¹⁸

In this chapter, we present a comprehensive micellar and thermodynamic study on the interaction between an anionic polyelectrolyte NaCMC and a cationic surface active ionic

liquid C₁₆MeImCl in aqueous media as a function of temperature as well as in presence of varying concentrations of NaCMC as probed by tensiometry and conductometry. The counterion-condensation behaviour of aqueous NaCMC in absence of C₁₆MeImCl, and the electrolyte and micellar behaviour of C₁₆MeImCl in absence of NaCMC has also been investigated to unravel the nature of NaCMC-C₁₆MeImCl interactions. Although the surface and micellar behaviour in NaCMC-conventional cationic surfactant systems is now well understood,¹⁹⁻²¹ that of NaCMC-C₁₆MeImCl system has not been investigated yet. Because of the greater ease of fine-tuning of the hydrophobicity of surface active ionic liquid molecules compared to their conventional counterparts, the interactions in NaCMC-surface active ionic liquid systems could be modulated conveniently in comparison with the NaCMC-conventional surfactant systems.

NaCMC is a chemically modified cellulose derivative with large water solubility, broadly used due to its low cost, lack of toxicity, and biodegradability. Food industry, cosmetics, pharmaceuticals, suspension agents, formulation agents in controlled release of drugs and pesticides, papers and paper products, adhesives, and ceramics provide a brief list of the numerous areas where carboxymethylcellulose is used in the acid or in the sodium salt form.²² It would, therefore, be interesting to study its interacting features with a surface active ionic liquids.

4.2 Experimental

NaCMC was purchased from Acros Organics. The average molecular weight of the sample was 90000 with a degree of substitution of 0.7. These values agree well with those obtained from physicochemical characterization in the present study. Fig. 4.1(a) presents the NaCMC X-ray diffraction (XRD) pattern, displays a broad peak at 20° associated with low crystallinity of NaCMC structure that has been previously observed.²³ C₁₆MeImCl, was purchased from Acros Organics and was used without further purification. Its purity was checked from tensiometric measurements as a function of concentration, and no minimum²⁴ was observed within the concentration range used in this work. The the XRD pattern of C₁₆MeImCl is shown in Fig. 4.1(b). The diffractogram is similar to that of another surface active ionic liquid sample 1-butyl-3-methylimidazolium chloride reported earlier²⁵ which also shows broad and small diffraction peaks.

Triply distilled water with a specific conductance of less than 10⁻⁶ S.cm⁻¹ at 298.15 K was used for the preparation of solutions.

XRD Measurements were carried out on a computer-controlled Rikagu diffractometer with a copper $K\alpha$ radiation ($\lambda = 0.15406$ nm) which was run at 40 kV and 40 mA.

The specific conductances (κ) were measured on a Thermo Scientific conductivity meter with a dip-type cell in a water thermostat maintained within 0.01 K of the desired temperature. Corrections were made for the specific conductance of solvents at all temperatures. The κ vs. $[C_{16}MeImCl]$ profile for NaCMC-free solution and that for a representative NaCMC-containing (concentration = 0.0005 monomol.L⁻¹) solution are depicted, respectively, in Figs. 4.2(a) and (b).

The surface tensions of the solutions (γ) were measured with a Krüss (Germany) K9 tensiometer by the platinum ring detachment method (uncertainty = $\pm 1 \times 10^{-3}$ N.m⁻¹). The tensiometer was connected to a water-flow cryostat in order to maintain the temperature equilibration. Prior to each measurement, the ring was briefly heated by holding it above a Bunsen burner until glowing. The γ vs. $[C_{16}MeImCl]$ profiles for polyelectrolyte-free solution and those for a polyelectrolyte-containing (NaCMC concentration = 0.0001 monomol.L⁻¹) solution are shown, respectively, in Figs. 4.2(c) and (d).

4.3 Results and Discussion

4.3.1 Ion-association Behaviour of Pure $C_{16}MeImCl$ (aq) in the Pre-micellar Regime

Conductometry provided important information on the ion-association behaviour of $C_{16}MeImCl$ below its critical micellar concentration (cmc) where it behaves as a 1-1 electrolyte. Such a knowledge would help understand its aggregation properties beyond cmc .

The molar conductance vs. concentration data below cmc have been analyzed by the Fuoss conductance-concentration equation²⁶ to derive the limiting molar conductivity (Λ^0), association constant (K_A), and the association diameter (R). Table 4.1 lists the Λ^0 , K_A , and R values along with the limiting equivalent conductances of Cl^- ($\lambda_{Cl^-}^0$) and Na^+ ions ($\lambda_{Na^+}^0$) at the experimental temperatures. The $\lambda_{Cl^-}^0$ and $\lambda_{Na^+}^0$ values at 298.15, 308.15, and 318.15 K have been taken from the literature.²⁷ Since the values at 303.15 and 313.15 K are not available, these were obtained by regressing the available literature²⁷ $\lambda_{Cl^-}^0$ or $\lambda_{Na^+}^0$ values as a function of temperature. The low K_A values of aqueous $C_{16}MeImCl$ indicates that a preponderant proportion of $C_{16}MeImCl$ remains as free ions over the temperature range investigated. A

comparison of the $\lambda_{\text{C}_{16}\text{MeIm}^+}^0$ and $\lambda_{\text{Na}^+}^0$ values reveals that the Na^+ ions are approximately 2.7-2.8 times more mobile than the $\text{C}_{16}\text{MeIm}^+$ ions within the investigated temperature range. It may, however, be pointed out that the $\lambda_{\text{C}_{16}\text{MeIm}^+}^0$ value at 298.15 K was also reported earlier by Vanyur *et al.*²⁸ But, their value (32 S.cm².mol⁻¹) does not at all agree with that obtained here. As a check, we computed the $\lambda_{\text{C}_{16}\text{MeIm}^+}^0$ value by subtracting the literature value²⁷ of $\lambda_{\text{Br}^-}^0$ from the Λ^0 of $\text{C}_{16}\text{MeImBr}$ in water at 298.15 K obtained as the intercept of the Λ vs. square root of the concentration data of aqueous $\text{C}_{16}\text{MeImBr}$ reported by Inoue *et al.*²⁹ The agreement of this computed value (*ca.* 16 S.cm².eqv⁻¹) with that obtained in the present work is very good.

4.3.2 Aggregation Behaviour of Pure $\text{C}_{16}\text{MeImCl}$ and its Thermodynamics

4.3.2.1 Tensiometry

Tensiometry records the threshold surfactant concentration required to saturate the air/solution interface as the *cmc* which is obtained from a sharp break in the γ versus [surfactant] profiles (*cf.* Fig. 4.2(c)). The *cmc* values of $\text{C}_{16}\text{MeImCl}$ in aqueous solutions at different temperatures are listed in Table 4.2. It is observed that the *cmc* of pure $\text{C}_{16}\text{MeImCl}$ increases with increasing temperature within the investigated temperature interval. The γ values upon complete air/solution interfacial saturation (γ_{cmc}) of pure $\text{C}_{16}\text{MeImCl}$ are also listed in Table 4.2; γ_{cmc} values are found to decrease slightly with temperature elevation.

The values of Gibbs surface excess (Γ_{max}), governing the efficacy of $\text{C}_{16}\text{MeImCl}$ molecules to be adsorbed at the interface as compared to the bulk phase, were calculated using the following equation:³⁰

$$\Gamma_{\text{max}} = -\frac{1}{nRT} \lim_{[\text{C}_{16}\text{MeImCl}] \rightarrow \text{cmc}} \left(\frac{\partial \gamma}{\partial \ln[\text{C}_{16}\text{MeImCl}]} \right)_{T,p} \quad (1)$$

where n is the number of species per surfactant monomer in solution, R the universal gas constant, and T the temperature in absolute scale. The Γ_{max} values thus obtained are reported in Table 4.2. A decrease in the Γ_{max} values with the rise in the temperature manifests an enhancement of the efficacy of the surfactant monomers to populate the interface at lower

temperatures. The area of exclusion per surfactant monomer was calculated assuming complete monolayer formation at *cmc* using the following equation:

$$A_{\min} = \frac{10^{18}}{N_A \Gamma_{\max}} \quad (2)$$

in $\text{m}^2 \cdot \text{molecule}^{-1}$, where N_A is the Avogadro's number. The values of A_{\min} are also listed in Table 4.2. The increase in the A_{\min} values with temperature may be ascribed to the greater kinetic motion of the monomers populating the air/water interface. From Table 4.2 one can notice that the values of Γ_{\max} decrease and those of A_{\min} increase, when the temperature of the system increases. It shows that the higher the temperature is, the weaker is the tendency of those molecules to escape from the solvent to the air/solvent, resulting in a less packed surface at elevated temperatures.

4.3.2.2 Conductometry

A sharp break in the κ vs. $[\text{C}_{16}\text{MeImCl}]$ isotherm corresponds to the onset of micellization in the bulk solution as shown in Fig. 4.2(a). Conductometric *cmc* values agree well with those obtained from tensiometry (*cf.* Table 4.2). Both conductometric and tensiometric *cmc*s are found to increase monotonically with temperature.

The degree of counterion binding (β) onto the self-aggregated assemblies was obtained from the slopes of the κ versus $[\text{C}_{16}\text{MeImCl}]$ isotherm in the premicellar region (S_1) and the postmicellar region (S_2) using the following relationship:

$$\beta = 1 - \frac{S_2}{S_1} \quad (3)$$

The β values, recorded in Table 4.2, decreased slightly with temperature.

The free energy change of the micellization process (ΔG_m^0) was calculated using the equation:

$$\Delta G_m^0 = (1 + \beta)RT \ln x_{\text{cmc}} \quad (4)$$

where x_{cmc} is the *cmc* of C₁₆MeImCl in mole fraction scale. The β factor includes the fraction of free energy required to condense the counterions on the aggregate to reduce the repulsion between the adjacent monomer head groups.³¹

The corresponding standard enthalpy change (ΔH_m^0) is given by

$$\Delta H_m^0 = -RT^2 \left[(1 + \beta) \left(\frac{\partial \ln x_{\text{cmc}}}{\partial T} \right)_p - \ln x_{\text{cmc}} \left(\frac{\partial \beta}{\partial T} \right)_p \right] \quad (5)$$

Since the temperature derivative of β for aqueous C₁₆MeImCl is found to be small over the temperature range investigated here, Eq. (5) can then be simplified to

$$\Delta H_m^0 = -(1 + \beta)RT^2 \left(\frac{\partial \ln x_{\text{cmc}}}{\partial T} \right)_p \quad (6)$$

The standard entropy of micellization (ΔS_m^0) was calculated from:

$$\Delta G_m^0 = \Delta H_m^0 - T\Delta S_m^0 \quad (7)$$

The ΔG_m^0 , ΔH_m^0 and $T\Delta S_m^0$ values for aqueous solutions of C₁₆MeImCl are listed in Table 4.2.

The decrease in the ΔH_m^0 values on increasing temperature implies the less enthalpy-controlled system at elevated temperatures.

The ΔG_m^0 values are found to be negative over the entire range of the temperatures studied for aqueous C₁₆MeImCl. This observation indicates a spontaneous process of micelle formation of this surface active ionic liquid in aqueous solution. The ΔH_m^0 and $T\Delta S_m^0$ values contribute oppositely to ΔG_m^0 , so the value of ΔG_m^0 is dependent on relative changes of enthalpy and entropy in the system. It is seen that the variations of enthalpy and entropy of micellization nearly compensate each other, and hence ΔG_m^0 is only slightly dependent on temperature.

The ΔS_m^0 values are positive over the whole temperature range of measurement and decrease with the rise of temperature. The positive entropy values indicate that the process of micellization of pure aqueous surface active ionic liquid is entropically driven. Entropy of

micellization - the principal driving force towards micelle formation - is initiated by the highly ordered arrangement of the water molecules around the hydrophobic domain of the surface active ionic liquid. The contributing factors to $T\Delta S_m^0$, are: (a) release of a substantial fraction of the water molecules "frozen" around the hydrophobic surfactant chains, (b) readjustment of the head-group in response to the charge density on the micellar surface caused by monomer association and counterion binding, (c) increase in the degrees of freedom of the surfactant molecules in the micelle, and (d) decrease in the degrees of freedom of the head-groups at the interface. The present results indicate an increase in the degrees of freedom of the system. With the increase in temperature, there is an attenuation in the contribution of entropy of micellization, because at higher temperatures water molecules around the hydrophobic core of the molecules become less organized.

Three important factors which contribute to the value of ΔH_m^0 are: (a) a positive contribution associated with the release of structural water molecules from the hydration layer around the hydrophilic domain, (b) an additional positive contribution arising from the release of water molecules from the water cage around the hydrophobic moiety of the surface active ionic liquids, and (c) a negative contribution associated with the transfer of the hydrocarbon chains into the micelle and restoration of the H-bonding structure of the water around the micelle. With increasing temperature the degree of H-bonding around the surface active ionic liquid molecules decreases, and therefore the energy required to break also diminishes. The experimental values indicate that the negative contribution predominates in aqueous solutions of C₁₆MeImCl over the investigated range of temperature, *i.e.*, micellization of C₁₆MeImCl in the aqueous solution is exothermic.

Table 4.2 reveals that while the ΔH_m^0 value is negative and becomes more negative with increasing temperature, the $T\Delta S_m^0$ values are, in general, positive and becomes less positive as temperature increases. These results demonstrate that the micellization of C₁₆MeImCl in aqueous solution is governed by the entropy-enthalpy compensation effect, and that it is driven by the positive entropy. Similar behaviour has also been observed previously by us for pure alkyltrimethylammonium bromides in the ethylene glycol-water mixed solvent media.³²

4.3.3 Counterion-condensation Behaviour of Pure NaCMC (aq)

Using the de Gennes scaling model for the configuration of a polyion chain, Colby³³ derived the following expression for the equivalent conductivity (Λ) of a polyelectrolyte solution as a function of concentration (c_p)

$$\Lambda = f \left[\lambda_c^0 + \frac{F|z_c|ec_p\xi_0^2}{3\pi\eta_0} \ln \left(\frac{\xi_0}{\xi_e} \right) \right] \quad (8)$$

where λ_c^0 is the counterion limiting equivalent conductivity, f the fraction of free counterions, F the Faraday number, z_c the counterion charge, e the electronic charge, η_0 the solvent viscosity coefficient, ξ_0 the correlation blob size and ξ_e the electrostatic blob size. This equation has been applied to the measured Λ vs. c_p data for aqueous NaCMC solutions to determine the fraction of free counterions.

Fig. 4.3 depicts the variation of f as a function of temperature in aqueous solutions with varying amounts of NaCMC. It is observed that *ca.* 71-75% of the counterions remain free in the aqueous NaCMC solutions within the concentration and temperature ranges investigated. The values of f are found to marginally increase as the polyelectrolyte concentration increases at any given temperature. As polyelectrolyte concentration increases, the relative permittivity of the medium (ϵ) is also known to increase, owing to the polarizability of polyelectrolytes.³⁴ While the increase in the effective relative permittivity of the medium is not completely understood yet,³⁵ the experimental evidence is well established,³⁶ For NaPSS, in particular, the frequency-dependent relative permittivity is known to increase with the polyelectrolyte concentration.³⁷ The increase in the ϵ of the medium would result in a decrease in the Bjerrum length defined as

$$\lambda_B = \frac{e^2}{\epsilon k_B T} \quad (9)$$

where k_B is the Boltzmann constant, and T the absolute temperature.

Since λ_B sets the length scale for the distance between the dissociated counterions on the polyion chain,^{34,38} there will be fewer condensed counterions as ϵ of the medium increases.

The fraction of free counterions is found to decrease slightly with increasing temperature for the three polyelectrolyte concentrations used in the present study. This can be ascribed to a change in solvation and condensation behaviour of counterions upon changing the temperature. Raising the temperature has the effect of gradual desolvation for the counterions and the polyions which results in an increase of counterion-condensation on the polyion chain. This is reflected in the decreasing fraction of free counterions at higher temperatures. Desolvation of the sodium counterions with increasing temperature is directly evident from our earlier investigation where we noted a significant increase in their mobility with temperature.³⁹ This might be ascribed to the decreasing size of their solvodynamic entity and hence an increasing surface charge density resulting in a greater mobility under the action of the applied electric field. A similar behaviour was also observed for aqueous solutions of sodium and potassium dextran sulfates⁴⁰ where an increase in the charge density parameter defined as the ratio of the Bjerrum length to the contour distance per unit charge on the polyion (and hence, according to Eq. (9), a decrease in the fraction of free counterions) was reported with the rise of temperature. Similar results were observed with NaCMC⁴¹ and NaPSS⁴² in mixed-solvent media earlier.

4.3.4 Aggregation Behaviour: C₁₆MeImCl (aq) in Presence of NaCMC

NaCMC(aq) has been shown to be surface inactive below a concentration of 7 g.L⁻¹.²⁰ The maximum concentration of NaCMC used in this study, however, is *ca.* 0.16 g.L⁻¹ which is much below the limiting concentration above which the surface activity of NaCMC is reported to be observed. Hence, surface activity of NaCMC has nothing to do with the observed complexity in the tensiometric profiles of NaCMC-C₁₆MeImCl systems. Furthermore, at such low NaCMC concentrations, complexity arising out of the polyion-polyion interactions was also considered to be absent.

The presence of NaCMC in C₁₆MeImCl solutions greatly modifies the tensiometric behaviour of the surfactant in solution. Typical surface tension profiles for the present NaCMC-C₁₆MeImCl system as surfactant concentration varies are complex in nature, as shown in the representative tensiogram, Fig. 4.2(d), in presence of 0.0001 monomol.L⁻¹ NaCMC, and clearly show the existence of a hump in the profile. In all cases, there is a pronounced lowering of surface tension at lower surfactant concentrations when the polyelectrolyte is initially introduced as compared with the polyelectrolyte-free case. It appears that adsorption of polyelectrolyte-surfactant complexes occurs at surfactant concentrations well below the

concentration at which the surfactant molecules on their own are expected to adsorb appreciably. The polyelectrolyte-surfactant complexes are formed by cooperative binding of surfactant monomers onto the polyelectrolyte backbone due to the existence of strong electrostatic forces among themselves. Because of the monomeric adsorption on the polyelectrolyte charged sites, the hydrophobicity of the complex increases as a whole, and the complexes populate the Langmuirian interface. The initial drop in the surface tension may, therefore, be attributed to the gradual formation of a *surface-active* complex consisting of surfactant monomers bound to the polyion backbone. The minima in the profiles indicate the characteristic concentration (critical aggregation concentration, *cac*) beyond which a *non-surface active* polyelectrolyte-micellar aggregate where the surfactant molecules cooperatively adsorb on the polyion backbone in the form of micelles to form a necklace-like structure. The formation of these complexes dislodges the *surface-active* polyelectrolyte-surfactant monomer complex to sink into the bulk from the interface; consequently the interface was stripped off the surface active species with an increase in the surface tension until the formation of the necklace-like structures was complete. Upon completion of this process, there is monomer build-up at the interface with further increase in the concentration of C₁₆MeImCl. This is associated with a decline in surface tension until free micelles started to form at a surfactant concentration referred to as the apparent critical micellar concentration (*cmc**) after which surface tension reaches a final constant value close to or slightly lower than the surface tension values attained after *cmc* in pure C₁₆MeImCl systems indicating minor improvement of the surface activity of C₁₆MeImCl in the presence of NaCMC beyond *cmc*. A similar behaviour was also reported earlier.^{8,43,44} The maximum in a tensiogram represents the concentration at which the polyion chains are saturated with the polyelectrolyte-induced aggregates which will be referred to as the polymer saturation concentration (*psc*). The values of *cac*, *psc*, and *cmc** values obtained from tensiometry are recorded in Table 4.3.

The conductometric profiles for C₁₆MeImCl (aq) in presence of 0.0005 monomol.L⁻¹ NaCMC as a function of C₁₆MeImCl concentration are shown in Fig. 4.2(b). Initially, there is a distinct ascending part with a lower slope (regime I) in the κ vs. [C₁₆MeImCl] plot. Analysis of the conductivity of aqueous NaCMC solutions indicated that *ca.* 73-75% of the counterions would remain free at a concentration of 0.0005 monomol.L⁻¹ NaCMC, Fig. 4.2(a). The addition of C₁₆MeImCl, which is almost fully dissociated (*cf.* Table 4.1), to NaCMC solution causes the C₁₆MeIm⁺ ions to bind (*a*) to the free polyionic sites of NaCMC,

and (b) to the polyionic sites with condensed-counterions causing further counterion dissociation. The concentrations of free Na^+ and Cl^- ions in solution would thereby increase with increasing added surfactant concentration causing an increase in the solution conductivity. This initial ascending part of the conductometric profile is followed by a relatively steep rise (regime II) upon further addition of $\text{C}_{16}\text{MeImCl}$. The inflection represents the critical aggregation concentration (*cac*) beyond which polyelectrolyte-induced surfactant aggregates are formed. In regime II, smaller surfactant micelles upon binding to the polyion chains release more Na^+ counterions as compared to regime I thus increasing the specific conductance gradient in the post-*cac* regime. The Na^+ ions alongwith the dissociated fraction of the Cl^- ions of the polyelectrolyte-induced micelles conduct electricity in this regime. After the complexation is over, build-up of the monomer concentration takes place as indicated by a drop in the surface tension value after *psc* in our tensiometric study. But, this region of monomer-accumulation could not be identified from conductivity measurements. This indicates that the value of $d\kappa/d[\text{C}_{16}\text{MeImCl}]$ during complexation is approximately the same as that during the accumulation of the monomer in solution. In regime II after *psc*, the free $\text{C}_{16}\text{MeIm}^+$ and Cl^- ions are responsible for current conduction. When the concentration of $\text{C}_{16}\text{MeImCl}$ reaches its *cmc* in presence of NaCMC, free micelles started forming and we obtain regime III with a lower slope than regime II. In this regime the unbound Cl^- ions, whose concentrations are increasing upon addition of $\text{C}_{16}\text{MeImCl}$, carry electricity. Similar specific conductance versus surfactant concentration profiles for DNA-cationic surfactant systems exhibiting three linear segments with gradually decreasing slopes where two distinct breaks are discernible have also been reported earlier.⁴⁵ Conductivity isotherms with lower complexity manifesting two linear sections with one inflection (*e.g.*, in aqueous NaPSS-alkyltrimethylammonium bromide⁴⁶ or in sodium dextran sulfate-dodecylpyridinium chloride system⁴³ and those with higher complexity showing up four linear portions with three inflections (*e.g.*, in aqueous NaCMC-cetyltrimethylammonium bromide solution¹⁶ are also available in the literature. It may, however, be noted that for aqueous NaCMC-cetyltrimethylammonium bromide solution, where three-break conductivity isotherm was reported, the slopes of the straight lines before and after the *psc* differ negligibly from each other. The lower complexity in the conductivity profiles of the NaCMC- $\text{C}_{16}\text{MeImCl}$ (aq) system observed here may be attributed to the predominance of the electrostatic interactions over the hydrophobic effect in presence of the highly charged polyions.

The values of cac and cmc^* obtained from conductometry are listed in Table 4.3. It is observed that the values of cac (both from tensiometry and conductometry), p_{sc} (only from tensiometry), and cmc^* (both from tensiometry and conductometry), values increase monotonically with increasing added NaCMC concentration at any given temperature. They are also found to increase with increasing temperature in presence of a given amount of NaCMC.

A slight increase in cac and p_{sc} with NaCMC concentration was observed (*cf.* Table 4.3).

The cmc and cmc^* values are found to increase with increasing amount of the added NaCMC at any given experimental temperature. This may be ascribed to the lowering in the concentration of free $C_{16}MeImCl$ molecules since more $C_{16}MeImCl$ molecules are required to saturate an increased amount of NaCMC.

The influence of temperature on the critical aggregation concentration (cac) can be interpreted on the basis of the temperature dependence of the charge density of the polyelectrolyte. Although the influence of ξ of NaCMC at different temperatures on the cac values is small, it is clearly discernible from Fig. 4.4 where cac values measured at different temperatures have been plotted as a function of ξ of NaCMC in presence of three different polyelectrolyte concentrations. The profiles demonstrate a slow rise in the cac values with the polyelectrolyte charge density for each NaCMC concentration. The observation can be accounted for in terms of electrostatics: an increase in the temperature causes an increase in the value of ξ . At elevated temperatures, the "local cmc ", needed for self-aggregation of the amphiphile on the polyion, is thus reached at a somewhat higher surfactant concentration, leading to an increased cac .

4.3.5 Thermodynamics of Micellization of $C_{16}MeImCl$ (aq) in Presence of NaCMC

The ΔG_m^0 of $C_{16}MeImCl$ in presence of NaCMC are, in all cases, found to be negative. In Fig. 4.5(a)-(d), the ΔG_m^0 values of $C_{16}MeImCl$ have been plotted as a function of added NaCMC concentration at different temperatures. Also included in this figure are the ΔG_m^0 values for NaCMC-free system. From this figure, it is seen that micellization becomes more spontaneous on addition of NaCMC at any given temperature, and that the spontaneity of micellization increases as the amount of added NaCMC increases. In presence of NaCMC, however, the micellization becomes less spontaneous upon an elevation of temperature.

Some characteristic features of the thermodynamic parameters are manifested in Fig. 4.5 (a)-(d), which are common to the polyelectrolyte-free and polyelectrolyte-containing C₁₆MeImCl systems studied. It is directly evident that the micellization processes of C₁₆MeImCl are always exothermic over the investigated range of temperatures, whether the system contains NaCMC or not, and that these processes become more exothermic at higher temperatures. The value of $-T\Delta S_m^0$, on the other hand, increases with the rise of temperature. The results indicate that the entropy terms override the influence of the ΔH_m^0 values in governing the negative ΔG_m^0 values of the C₁₆MeImCl micellization processes both in absence as well as in the presence of NaCMC, *i.e.*, the micelle formation process for the investigated surface active ionic liquids is always entropy-driven. Similar behaviour has also been observed previously by us for pure alkyltrimethylammonium bromides in the ethylene glycol-water mixed solvent media.⁴⁷ However, the entropy term ($-T\Delta S_m^0$) becomes less negative, and the enthalpy term becomes more negative with the increase in temperature, but the former always being the predominant contributor to the free energy of the micellization processes for the system under investigation.

Lumry and Rajender⁴⁸ suggested that important information on the bulk structural property of aqueous solutions can be obtained from a linear correlation between ΔH_m^0 and ΔS_m^0 (enthalpy-entropy compensation). Such correlation can be generally described by the relation

$$\Delta H_m^0 = \Delta H_m^* + T\Delta S_m^0 \quad (10)$$

where T_c is the compensation temperature, and ΔH_m^* is the corresponding intercept. T_c has been proposed as a measure of the “hydration part” of the micellization process (dehydration of the hydrophobic chains).⁴⁶ ΔH_m^* provides information on the solute-solute interactions and is considered as an index of the “chemical part” of micelle formation (association of the non-polar chains to form a micellar unit). T_c for the micellization process of aqueous C₁₆MeImCl is found to be 280 K. It was suggested that this value in aqueous solution was expected to lie between 270 and 294 K for processes dominated by hydration.^{48,49} Our observed value for aqueous solution of C₁₆MeImCl is, thus, well within this stipulated range. Here micellization depends upon the bulk structure of the solvent. The T_c values are found to decrease with the addition of NaCMC to aqueous C₁₆MeImCl solution. T_c value in presence of 0.00001 monomol.L⁻¹ NaCMC (275 K) lies between 270 and 294 K. This means that the micellization

process in this system is still governed by the same structural property of pure water, and the presence of NaCMC only has a minor effect on the solute-solvent interactions. However, the variations observed in presence of 0.0001 and 0.0005 monomol.L⁻¹ NaCMC as well as those observed earlier⁵¹ may be due to the difference of the bulk structural property of the solution from that of the water. It is, however, worth mentioning that the linearity in ΔH_m^0 vs. ΔS_m^0 plots should not be overinterpreted,⁵² though this linearity is quite often seen.

4.4 Conclusions

The interaction of NaCMC with C₁₆MeImCl was studied in aqueous solution using conductometry and tensiometry. The ion-association behaviour of C₁₆MeImCl (aq) in the premicellar regime, and the counterion-condensation behaviour of NaCMC (aq) was also investigated. Approximately 71-75% of the counterions remain free in the aqueous NaCMC solutions within the NaCMC concentration and temperature ranges investigated. The results indicated the formation of *surface-active* complexes consisting of surfactant monomers bound to the polyion backbone, and *non-surface active* necklace-like polyion-micellar aggregates in NaCMC-C₁₆MeImCl solutions. This process exhibited a minimum, referred to as the critical aggregation concentration, in the tensiogram which marks the boundary between the formation of these two species with different surface activities. The concentration at which the polyion chains are saturated with the polyelectrolyte-bound micellar aggregates, referred to as the polymer saturation concentration, has been identified as a maximum in the tensiogram beyond critical aggregation concentration. In C₁₆MeImCl-NaCMC system, free C₁₆MeImCl micelles appear above the apparent critical micellization concentration, which is appreciably higher than the ordinary critical micellization concentration in pure C₁₆MeImCl solutions. The thermodynamic parameters for micelle formation of aqueous C₁₆MeImCl were estimated both in absence and in the presence of NaCMC. The contribution of the entropy terms to the free energy of micellization always predominates over that of the enthalpy terms. The enthalpy-entropy compensation effect in C₁₆MeImCl and NaCMC-C₁₆MeImCl systems provided important insight as to how micellization processes are governed by the bulk structural property of the solution with respect to that of the water. The variation of the aggregation behaviour of C₁₆MeImCl with varying amounts of added NaCMC as demonstrated in the present study, would be expected to modulate the antimicrobial activity of C₁₆MeImCl since the antimicrobial activity of surface active ionic liquids is greatly influenced by their aggregation behaviour. The present results might, therefore, initiate further studies on the antimicrobial activity of C₁₆MeImCl in

presence of NaCMC in assessing the possible role of polyelectrolytes in modulating the antimicrobial activity of surface active ionic liquids.

4.5 References

1. E. D. Goddard, *J. Colloid Interface Sci.*, **256**, 228 (2001).
2. B. Jönsson, B. Lindman, K. Holmberg, and B. Kronberg, *Surfactants and Polymers in Aqueous Solution*, John Wiley and Sons, London (1998).
3. K. Kogez, *Adv. Colloid Interface Sci.*, **158**, 68 (2010).
4. C. Wandrey, D. Hunkeler, In *Handbook of Polyelectrolytes and Their Applications*, S. K. Tripathy, J. Kumar, H. S. Nalwa (Eds.), Vol 2, p. 147, American Scientific Publishers, Stevenson Ranch, CA (2002).
5. J. C. T. Kwak, *Surfactant Science Series*, Vol. 77, *Polymer–Surfactant Systems*, Marcel Dekker, NY (1998).
6. B. Lindman, and K. Thalberg, In *Interaction of Surfactants with Polymers and Proteins*, E. D. Goddard, K. P. Ananthapadmanabhan (Eds.), Chapter 5, CRC Press, Boca Raton, FL (1993).
7. T. Nylander, Y. Samoshina, and B. Lindman, *Adv. Colloid Interface Sci.*, **123**, 105 (2006).
8. D. J. F. Taylor, R. K. Thomas, P. X. Li, and J. Penfold, *Langmuir*, **19**, 3712 (2003).
9. J. L. Anderson, V. Pino, E. C. Hagberg, V. V. Sheares, and D. W. Armstrong, *Chem. Commun.*, **19**, 2444 (2003).
10. M. Ao, P. Huang, G. Xu, X. Yang, and Y. Wang, *Colloid. Polym. Sci.*, **287**, 395 (2009).
11. M. Blesic, M. Marques, N. V. Plechkova, K. R. Seddon, L. P. N. Rebelo, and A. Lopes, *Green Chem.*, **9**, 481 (2007).
12. A. Cornellas, L. Perez, F. Comelles, I. Robosa, A. Manresa, and M. T. Garcia, *J. Colloid Interface Sci.*, **355**, 164 (2011).
13. P. D. Galgano, and O. A. El Seoud, *J. Colloid Interface Sci.*, **345**, 1 (2010).
14. T. Inoue, H. Ebina, B. Dong, and L. Zheng, *J. Colloid Interface Sci.*, **314**, 236 (2007).
15. J. Luczak, J. Hupka, J. Thoming, and C. Jungnickel, *Colloids Surf. A*, **329**, 125 (2008).
16. T. Singh, and A. Kumar, *J. Phys. Chem. B*, **111**, 7843 (2007).
17. R. Vanyúr, L. Biczók, and Z. Miskolczy, *Colloids Surf. A*, **299**, 256 (2007).
18. J. Luczak, C. Jungnickel, I. Lacka, S. Stolte, and J. Hupka, *Green Chem.*, **12**, 593 (2010).
19. T. Chakraborty, I. Chakraborty, and S. Ghosh, *Langmuir*, **22**, 9905 (2006).

20. S. Guillot, M. Delsanti, S. Desert, and D. Langevin, *Langmuir*, **19**, 230 (2003).
21. N. Jain, S. Trabelsi, S. Guillot, D. Mc Loughlin, D. Langevin, P. Letellier, and M. Turmine, *Langmuir*, **20**, 8496 (2004).
22. E. K. Just, and T. G. Majewicz, *Encyclopedia of Polymer Science and Engineering*, 2nd ed., John Wiley and Sons, NY (1985).
23. J. Shang, Z. Shao, and X. Chen, *Biomacromolecules*, **9**, 1208 (2008).
24. M. Blesic, M. Marques, N. V. Plechkova, K. R. Seddon, L. P. N. Rebelo, and A. Lopes, *Green Chem.*, **9**, 481 (2007).
25. J. Kadokawa, M. Murakami, T. Akihiko, and Y. Kaneko, *Carbohydr. Polym.*, **75**, 180 (2009).
26. R. M. Fuoss, *J. Phys. Chem.*, **82**, 2427 (1978).
27. R. A. Robinson, and R. H. Stokes, *Electrolyte Solutions*, 2nd ed., Butterworths, London (1959).
28. R. Vanyúr, L. Biczók, and Z. Miskolczy, *Colloids Surf. A*, **299**, 256 (2007).
29. T. Inoue, H. Ebina, B. Dong, and L. Zheng, *J. Colloid Interface Sci.*, **314**, 236 (2007).
30. M. J. Rosen, *Surfactants and Interfacial Phenomena*, 2nd ed., Wiley-Interscience, NY (1989).
31. G. Gunnarsson, J. Jönsson, and H. Wennerström, *J. Phys. Chem.*, **84**, 3114 (1980).
32. C. Das, and B. Das, *J. Chem. Eng. Data*, **54**, 559 (2009).
33. R. H. Colby, D. C. Boris., W.E. Krause, and J. S. Tan, *J. Polym. Sci., Part B: Polym. Phys.*, **35**, 2951 (1997).
34. F. Oosawa, *Polyelectrolytes*, Marcel Dekker, NY (1971).
35. U. Mohanty, and Y. Zhao, *Biopolymers*, **38**, 377 (1996).
36. M. Mandel, and T. Odijk, *Ann. Rev. Phys. Chem.*, **35**, 75 (1984).
37. F. Van der Touw, and M. Mandel, *Biophysical Chem.*, **2**, 231 (1974).
38. G. S. Manning, *J. Chem. Phys.*, **51**, 934 (1969).
39. A. Chatterjee, and B. Das, *J. Chem. Eng. Data*, **51**, 1352 (2006).
40. P. Beyer, and E. Nordmeier, *Eur. Polym. J.*, **31**, 1031 (1995).
41. A. Chatterjee, B. Das, and C. Das, *Carbohydr. Polym.*, **87**, 1144 (2012).
42. D. Ghosh, A. Bhattarai, and B. Das, *Colloid Polym. Sci.*, **287**, 1005 (2009).

43. D. F. Anghel, D. M. Mihai, G. Stinga, A. Iovescu, A. Baran, and R. V. Klitzing, *Rev. Roum. de Chem.*, **52**, 781 (2007).
44. E. Staples, I. Tucker, J. Penfold, N. Warren, R. K. Thomas, and D. J. F. Taylor, *Langmuir*, **18**, 5147 (2002).
45. R. S. Dias, L. M. Magno, A. J. M. Valente, D. Das, P. K. Das, S. Maiti, M.G. Miguel, and B. Lindman, *J. Phys. Chem. B*, **112**, 14446 (2008).
46. K. Kogez, and J. Skerjanc, *Langmuir*, **15**, 4251 (1999).
47. R. H. Colby, D. C. Boris., W.E. Krause, and J. S. Tan, *J. Polym. Sci., Part B: Polym. Phys.*, **35**, 2951 (1997).
48. R. Lumry, and S. Rajender, *Biopolymers*, **9**, 1125 (1970).
49. S. B. Sulthana, S. G. T. Bhat, and A. K. Rakshit, *Langmuir* 1997, **13**, 4562 (1997).
50. H. L. Friedman, and C.V. Krishnan, *J. Solution Chem.*, **2**, 119 (1973).
51. B. Sharma, and A. K. Rakshit, *J. Colloid Interface Sci.*, **129**, 139 (1989).
52. R. R. Krug, W. C. Hunter, and R. A. Grieger, *J. Phys. Chem.*, **80**, 2335 (1976).

TABLE 4.1. Conductance Parameters of C₁₆MeImCl in the Premicellar Regime along with the $\lambda_{\text{Cl}^-}^0$, $\lambda_{\text{C}_{16}\text{MeIm}^+}^0$, and $\lambda_{\text{Na}^+}^0$ values in Water at 298.15, 303.15, 308.15, 313.15, and 318.15 K.

T (K)	Λ^0 (S.cm ² . eqv ⁻¹)	K_A (dm ³ . mol ⁻¹)	$10^8 R$ (cm)	σ %	$\lambda_{\text{Cl}^-}^0$ (S.cm ² . eqv ⁻¹)	$\lambda_{\text{C}_{16}\text{MeIm}^+}^0$ (S.cm ² . eqv ⁻¹)	$\lambda_{\text{Na}^+}^0$ (S.cm ² . eqv ⁻¹)
298.15	95.16	26.71	7.16	0.14	76.35	18.81	50.10
303.15	104.82	26.50	7.20	0.35	84.38	20.44	55.80
308.15	115.00	26.48	7.25	0.65	92.21	22.79	61.54
313.15	123.47	26.44	7.30	0.30	100.42	23.05	67.61
318.15	135.01	27.02	7.35	0.39	108.92	26.09	73.73

TABLE 4.2. Critical Micellar Concentrations (*cmc*) and Related Thermodynamic Parameters for Pure C₁₆MeImCl in Aqueous Solutions at 298.15, 303.15, 308.15, 313.15, and 318.15 K.

<i>T</i> (K)	<i>cmc</i> (mM)			γ_{cmc} (mN.m ⁻¹)	Γ_{max} x 10 ⁶ (mol. m ⁻²)	A_{min} x 10 ¹⁸ (m ²)	β	ΔG_{m}^0 (kJ. mol ⁻¹)	ΔH_{m}^0 (kJ. mol ⁻¹)	$T\Delta S_{\text{m}}^0$ (kJ. mol ⁻¹)
	surf.	cond.	av.							
298.15	0.955	0.876	0.916	45.96	2.04	0.814	0.50	-40.94	-6.94	34.00
303.15	0.971	0.942	0.957	45.78	2.04	0.814	0.49	-41.16	-9.40	31.76
308.15	1.017	0.949	0.983	44.80	1.99	0.834	0.48	-41.48	-11.99	29.49
313.15	1.093	0.995	1.044	44.38	1.92	0.865	0.47	-41.60	-14.69	26.91
318.15	1.167	1.063	1.115	43.60	1.80	0.922	0.46	-41.75	-17.52	24.23

TABLE 4.3. Critical Micellar Aggregation Concentrations (cmc^*) of C₁₆MeImCl in Presence of Varying Concentration of Added NaCl Alongwith Critical Aggregation Concentrations (cac), Polymer Saturation Concentrations (psc) in Aqueous Solutions at 298.15, 303.15, 308.15, 313.15, and 318.15 K

T (K)	c (mono mol.L ⁻¹)	Method	cac (mM)	$av. cac$ (mM)	psc mM	$cmc^*/$ (mM)	$av. cmc^*$ (mM)
298.15	0.00001	Conductometry	0.148	0.151	-	0.981	1.035
		Tensiometry	0.154		0.254	1.089	
	0.00010	Conductometry	0.203	0.204	-	1.042	1.098
		Tensiometry	0.204		0.374	1.154	
	0.00050	Conductometry	0.478	0.479	-	1.419	1.355
		Tensiometry	0.480		0.596	1.291	
303.15	0.00001	Conductometry	0.170	0.173	-	0.989	1.048
		Tensiometry	0.175		0.272	1.106	
	0.00010	Conductometry	0.238	0.234	-	1.054	1.120
		Tensiometry	0.229		0.394	1.185	
	0.00050	Conductometry	0.485	0.480	-	1.421	1.368
		Tensiometry	0.474		0.617	1.315	
308.15	0.00001	Conductometry	0.186	0.185	-	1.007	1.072
		Tensiometry	0.183		0.327	1.137	
	0.00010	Conductometry	0.243	0.238	-	1.069	1.141
		Tensiometry	0.233		0.419	1.213	
	0.00050	Conductometry	0.490	0.495	-	1.441	1.397
		Tensiometry	0.500		0.642	1.352	

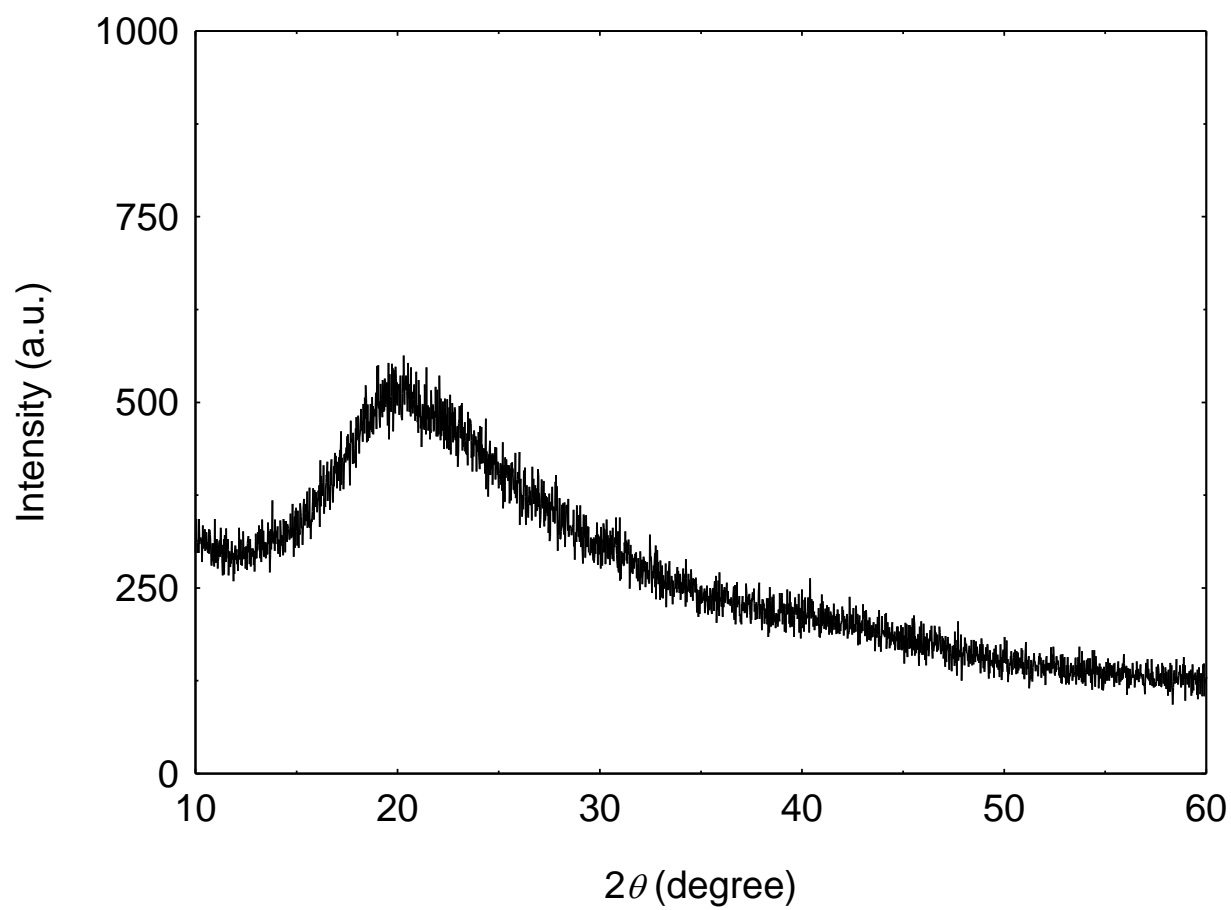


Fig. 4.1(a). XRD pattern of NaCMC.

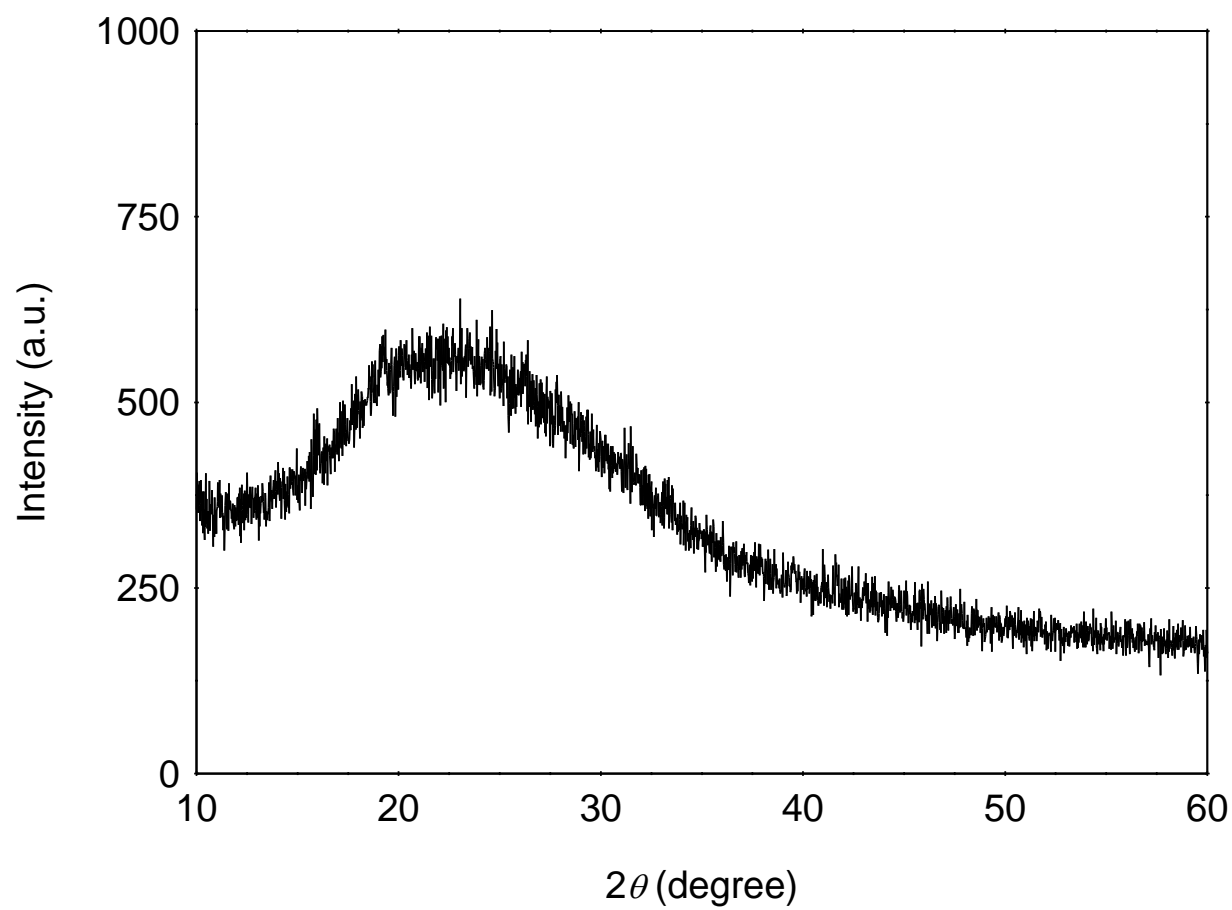


Fig. 4.1(b). XRD pattern of $\text{C}_{16}\text{MeImCl}$.

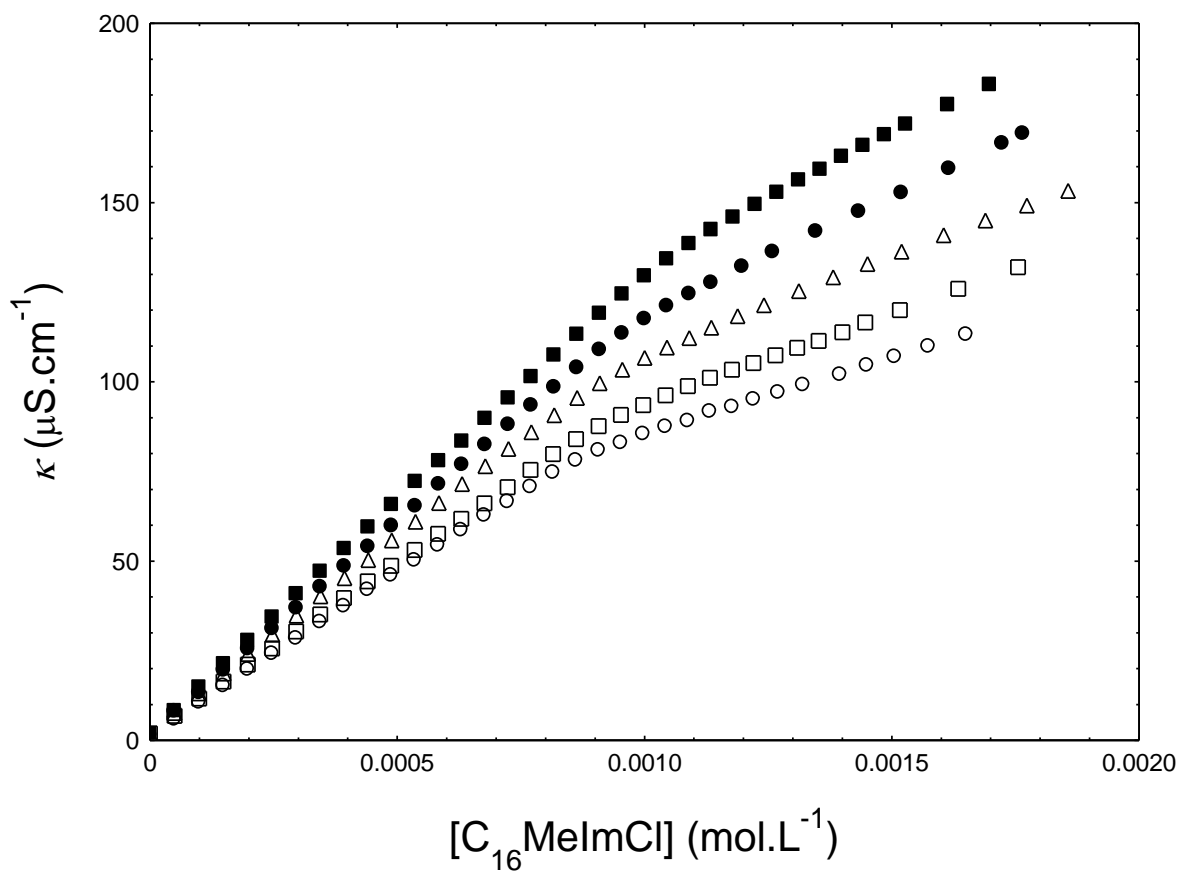


Fig. 4.2(a). Specific conductance (κ) vs. $[\text{C}_{16}\text{MeImCl}]$ profiles for $\text{C}_{16}\text{MeImCl}$ in water, at different temperature 298.15 K (\circ), 303.15 K (\square), 308.15 K (Δ), 313.15 K (\bullet), and 318.15 (\blacksquare).

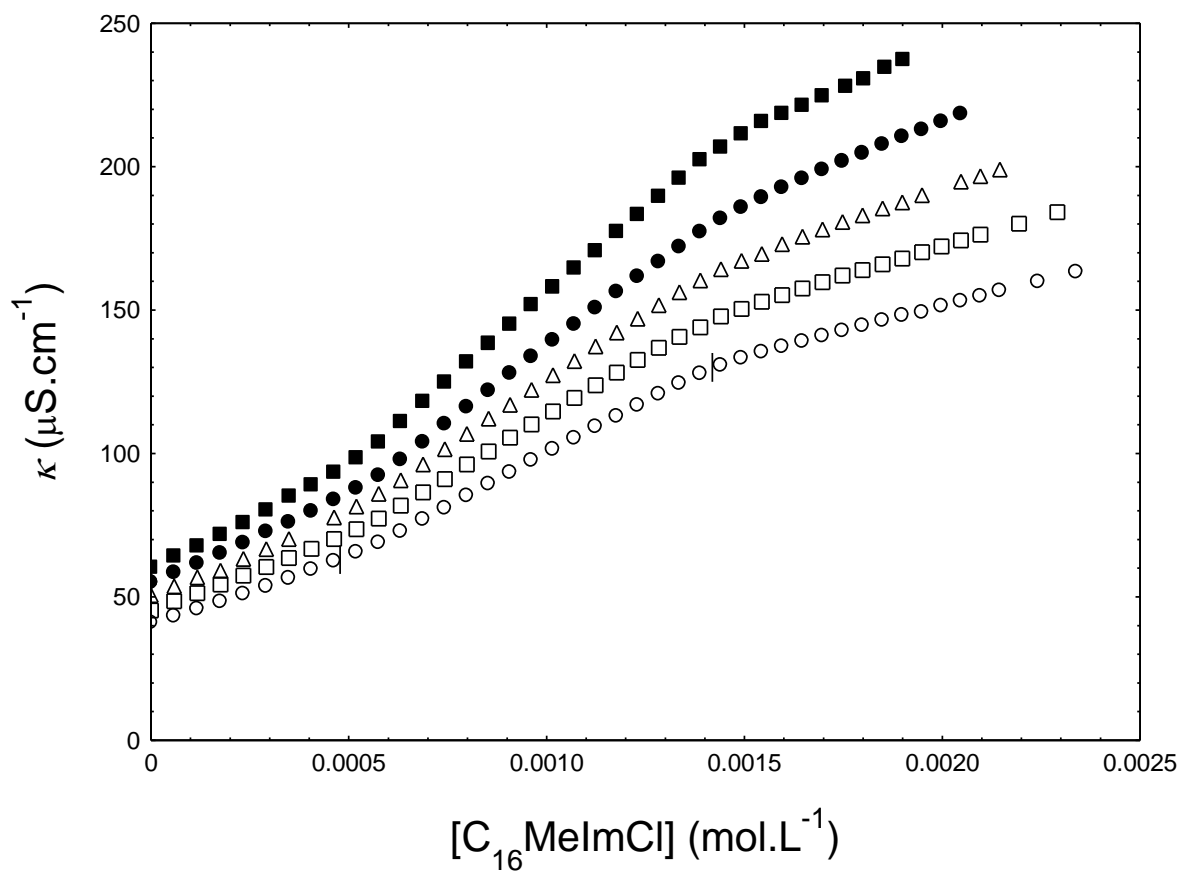


Fig. 4.2(b). Specific conductance (κ) vs. $[\text{C}_{16}\text{MeImCl}]$ profiles for $\text{C}_{16}\text{MeImCl}$ in presence of $0.0005 \text{ mol.L}^{-1}$ of aqueous NaCMC. Symbols: 298.15 K (\circ), 303.15 K (\square), 308.15 K (Δ), 313.15 K (\bullet), and 318.15 K (\blacksquare).

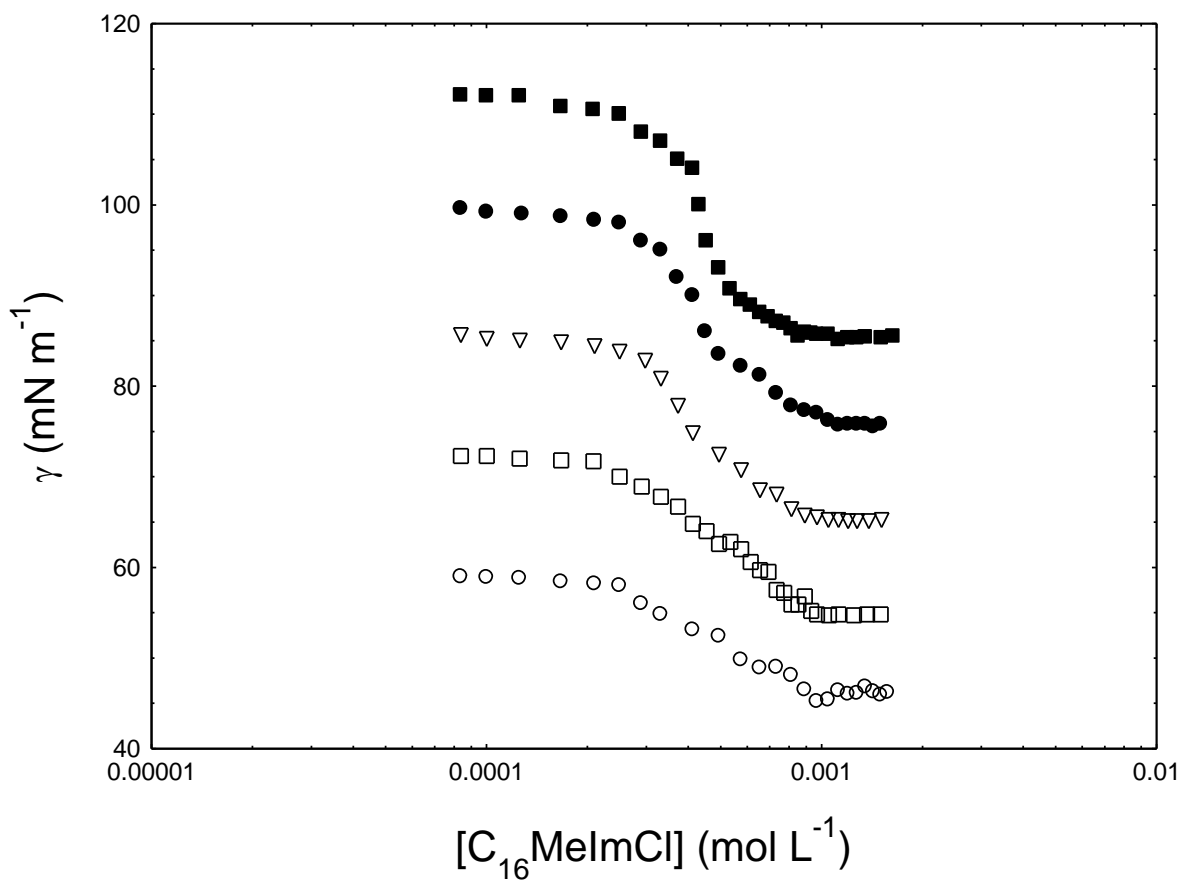


Fig. 4.2(c). Surface tension (γ) vs. $[\text{C}_{16}\text{MeImCl}]$ profiles for $\text{C}_{16}\text{MeImCl}$ in water. Symbols: 298.15 K (\circ), 303.15 K (\square), 308.15 K (Δ), 313.15 K (\bullet), and 318.15 (\blacksquare). The tensiometric isotherms have been offset vertically by 20 mN.m^{-1} for clarity.

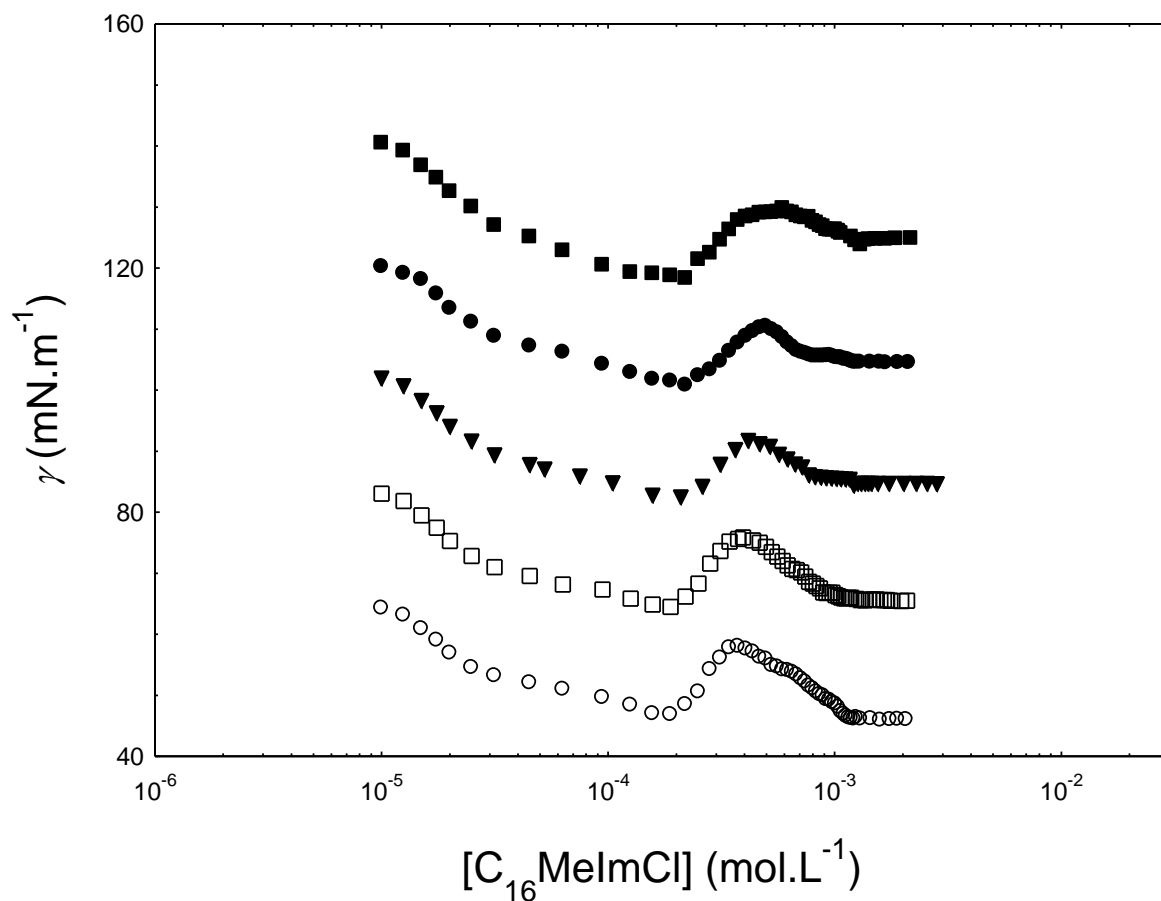


Fig. 4.2(d). Surface tension (γ) vs. $[\text{C}_{16}\text{MeImCl}]$ profiles for $\text{C}_{16}\text{MeImCl}$ in presence of $0.0001 \text{ mol.L}^{-1} \text{NaCMC}$. Symbols: 298.15 K (\circ), 303.15 K (\square), 308.15 K (Δ), 313.15 K (\bullet), and 318.15 K (\blacksquare). The tensiometric isotherms have been offset vertically by 20 mN.m^{-1} for clarity.

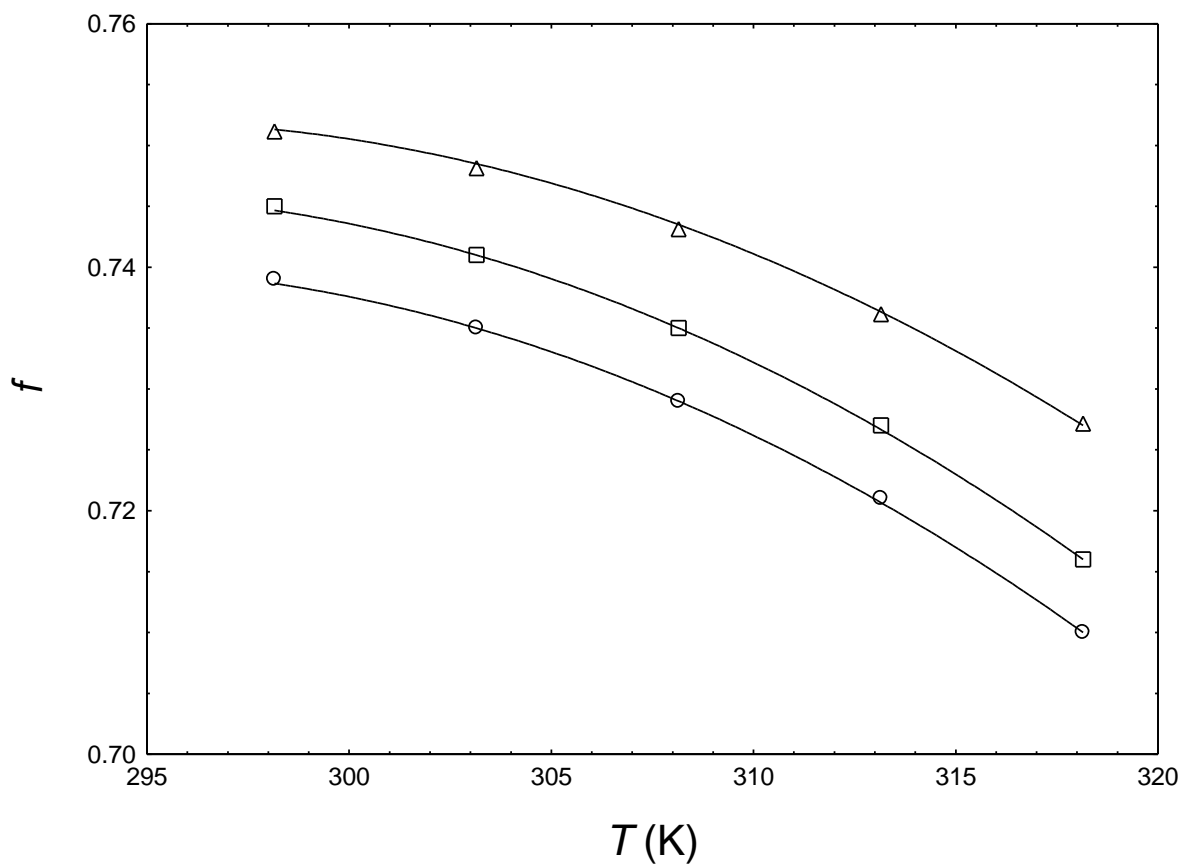


Fig. 4.3. Effect of temperature and concentration on the fraction of free counterions in aqueous solutions of NaCMC: 0.00001 monomol.L⁻¹(○), 0.0001 monomol.L⁻¹ (□), 0.0005 monomol.L⁻¹ (Δ).

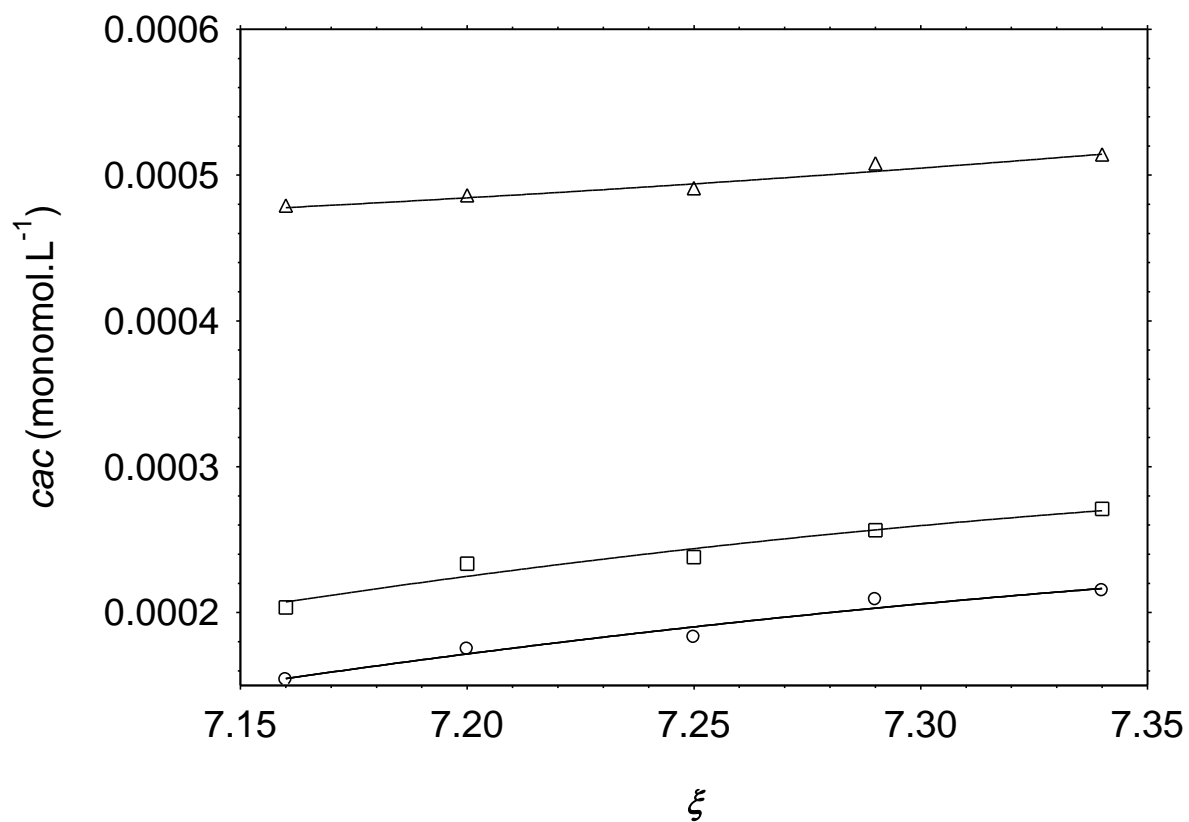


Fig. 4.4. Effect of the charge density of NaCMC on the cac in aqueous $C_{16}MeImCl$ solution in the presence of varying concentrations of NaCMC: 0.00001 monomol.L⁻¹ (\circ), 0.0001 monomol.L⁻¹ (\square), 0.0005 monomol.L⁻¹ (Δ).

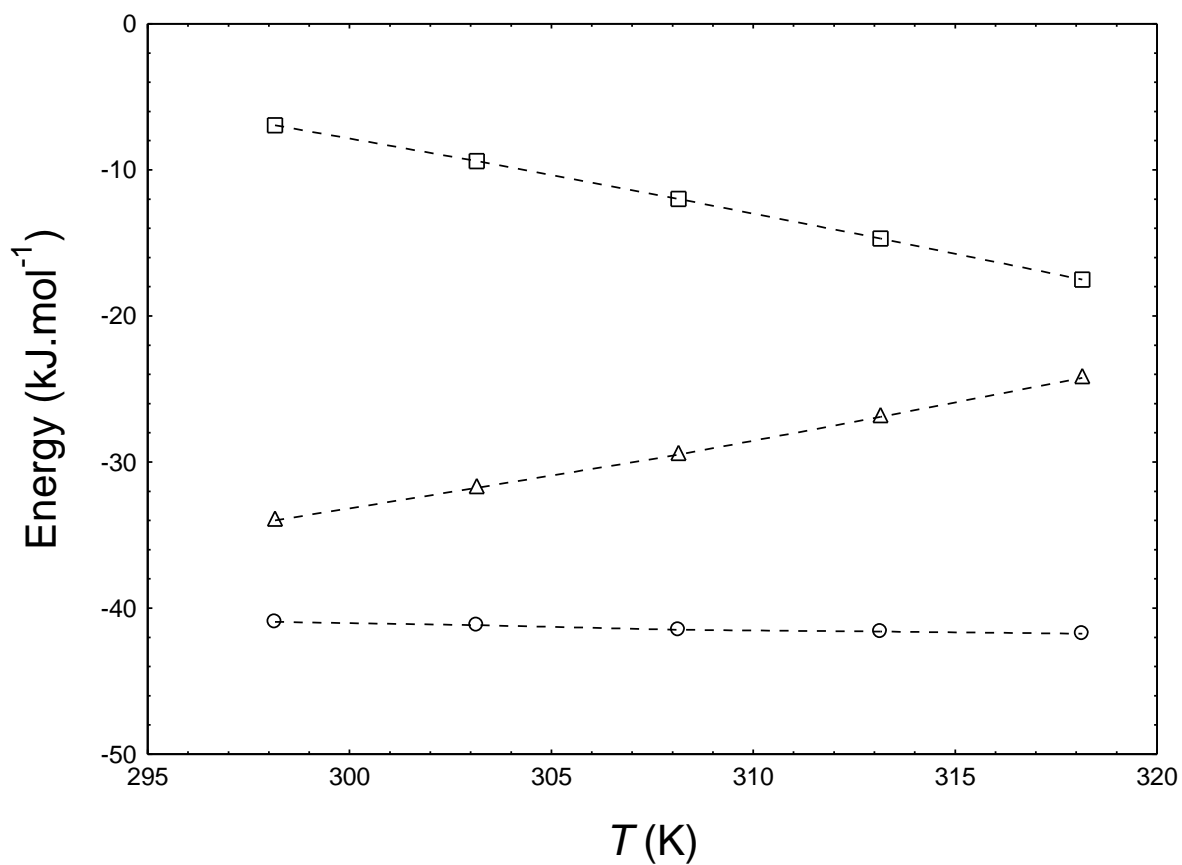


Fig. 4.5(a). Thermodynamic parameters of micellization of C₁₆MeImCl in water at different temperatures: ΔG_m^0 (\circ), ΔH_m^0 (\square), $-T\Delta S_m^0$ (Δ).

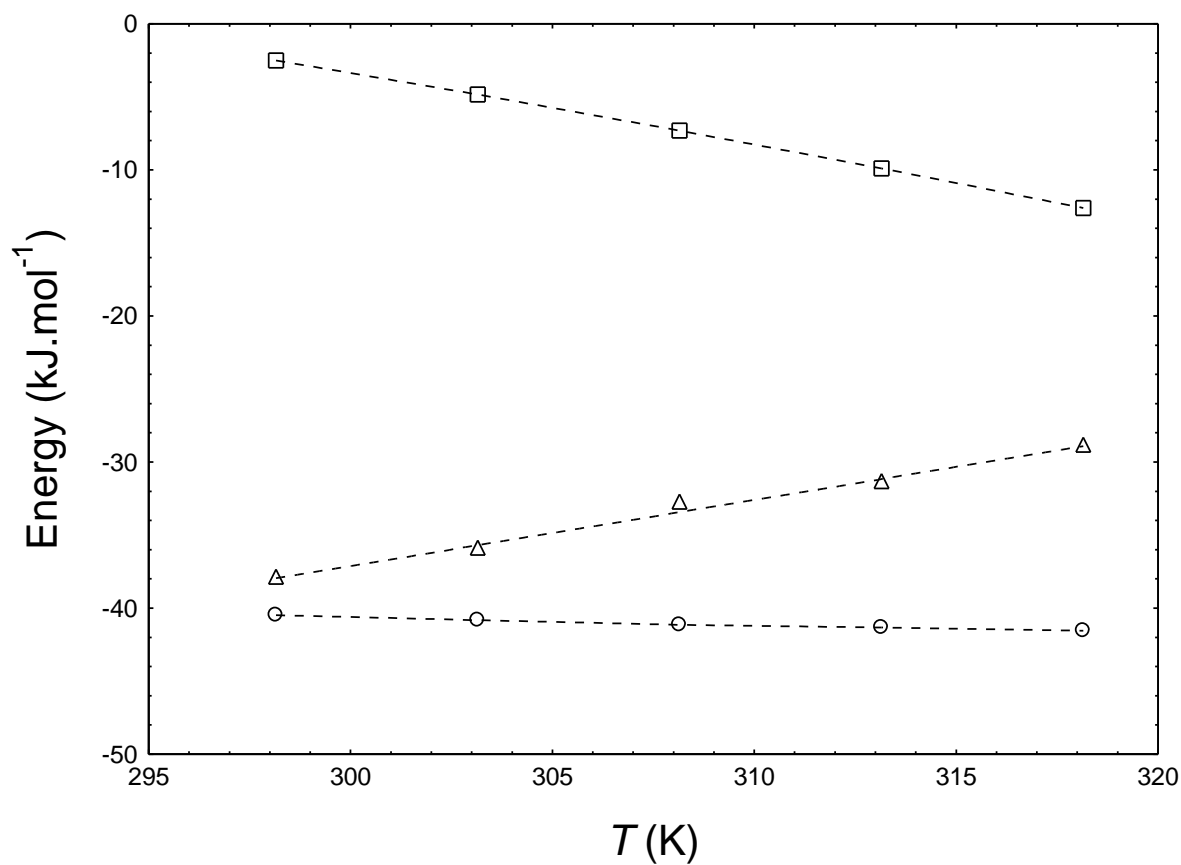


Fig. 4.5(b). Thermodynamic parameters of micellization of C₁₆MeImCl in presence of 0.00001 monomol.L⁻¹ of NaCMC (aq) at different temperatures: ΔG_m^0 (\circ), ΔH_m^0 (\square), $-T\Delta S_m^0$ (Δ).

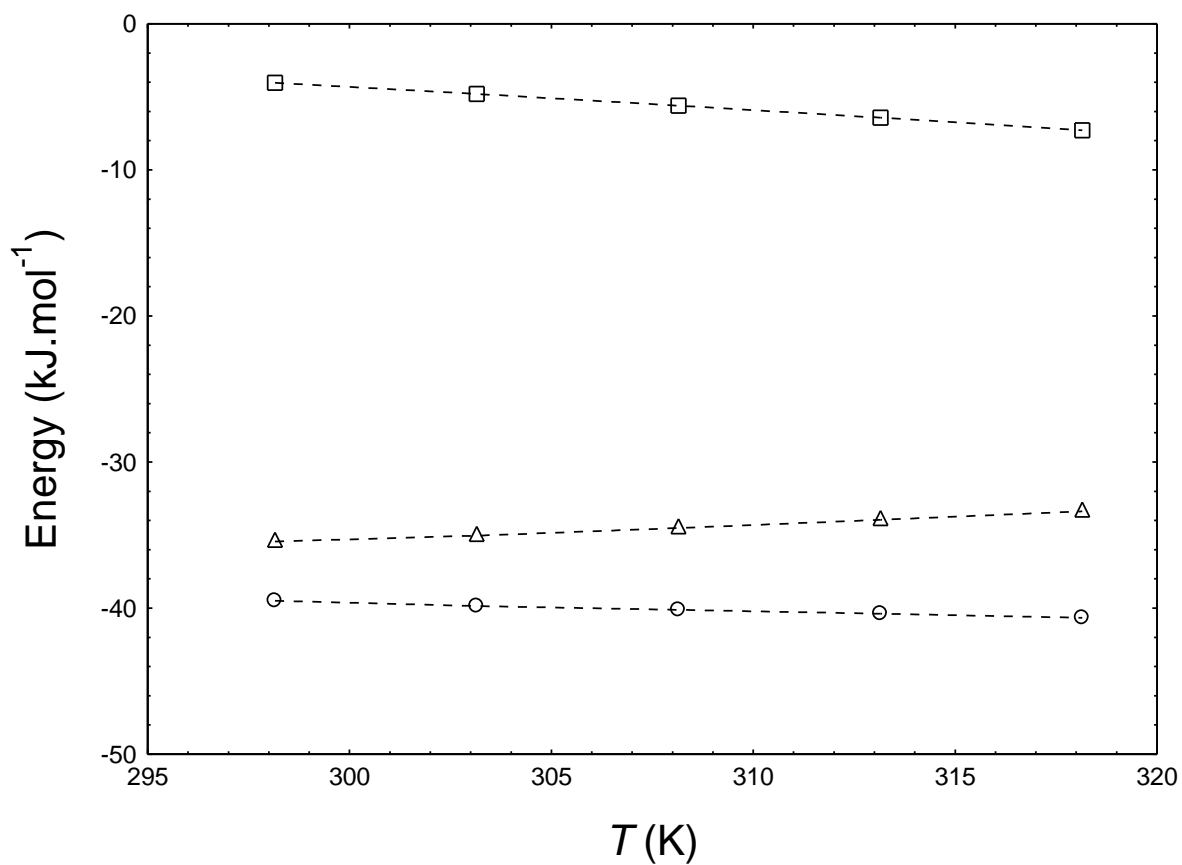


Fig. 4.5(c). Thermodynamic parameters of micellization of $C_{16}MeImCl$ in presence of $0.00005 \text{ monomol.L}^{-1}$ of $NaCMC \text{ (aq)}$ at different temperatures: ΔG_m^0 (\circ), ΔH_m^0 (\square), $-T\Delta S_m^0$ (Δ).

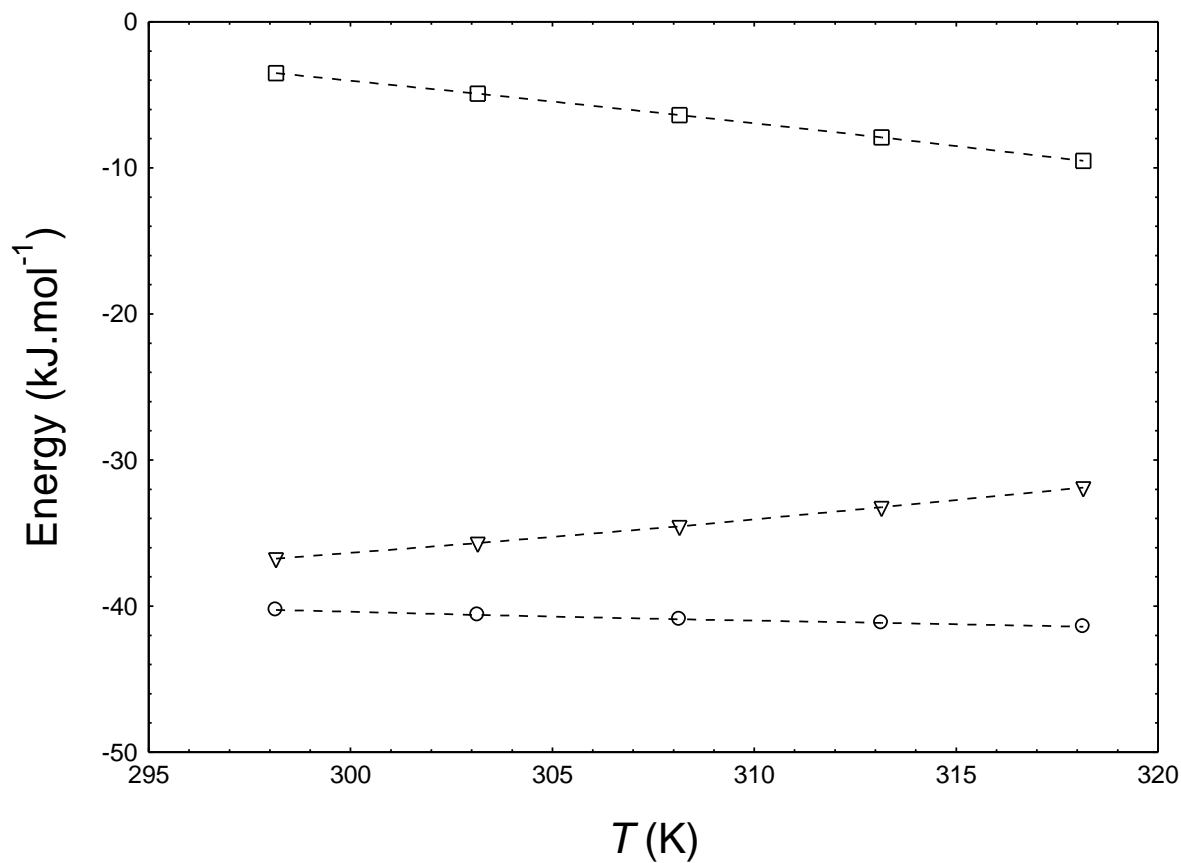


Fig. 4.5(d). Thermodynamic parameters of micellization of $C_{16}MeImCl$ in presence of $0.00010 \text{ monomol.L}^{-1}$ of $NaCMC \text{ (aq)}$ at different temperatures: ΔG_m^0 (\circ), ΔH_m^0 (\square), $-T\Delta S_m^0$ (Δ).